COAXIAL ELECTROSPRAYING OF BIOPOLYMERS AS A STRATEGY TO IMPROVE PROTECTION OF BIOACTIVE FOOD INGREDIENTS

*Laura G. Gómez-Mascaraque, Fran Tordera, Maria Jose Fabra, Marta Martínez-Sanz, Amparo Lopez-Rubio**

Food Safety and Preservation Department, IATA-CSIC, Avda. Agustín Escardino 7, 46980 Paterna, Valencia, Spain

*Corresponding author: Tel.: +34 963900022; fax: +34 963636301

E-mail address: amparo.lopez@iata.csic.es (A. López-Rubio)

ABSTRACT

Coaxial electrospraying is a promising technique for the production of multilayer encapsulation structures whose potential has already been demonstrated for pharmaceutical and biomedical applications. The aim of this work was to extend its application to the food sector by developing novel coaxially electrosprayed microcapsules using all food-grade materials. For this purpose, zein and gelatin were used as shell biopolymers to microencapsulate two model bioactive ingredients, i.e. epigallocatechin gallate (EGCG) as a model hydrophilic compound and α-linolenic acid (ALA) as a model hydrophobic molecule. The performance of the coaxially-obtained particles in terms of protection was evaluated in comparison with that of uniaxially electrosprayed materials. Particle sizes varied with composition and encapsulation efficiency (EE) was dependent on the chemical affinity between the shell matrix and the bioactive compound, but in general, greater EE was obtained in the coaxial systems. Moreover, enhanced bioactive protection ability was demonstrated by the coaxial structures, as observed in thermal degradation assays (for ALA) and antioxidant activity after *in-vitro* digestion (for EGCG).

INDUSTRIAL RELEVANCE: This work emphasizes the usefulness of the electrospraying technique for the production of encapsulation structures for bioactive protection using all food-grade materials, without the need of applying high temperatures and generating small capsule sizes (in the submicron range). It also demonstrates that the coaxial configuration may be used to design encapsulation systems with enhanced protection ability for both hydrophilic and hydrophobic bioactive compounds.

Keywords

Microencapsulation; Coaxial electrospraying; Food proteins; omega-3 fatty acid; green tea catechins

1. INTRODUCTION

Electrohydrodynamic techniques, including electrospinning and electrospraying, have gained, in the last years, increased interest as encapsulation techniques for a broad range of compounds. The formation of encapsulation structures through electrohydrodynamic processes is based on applying a strong external electrical field between a polymeric or biopolymeric solution and a grounded collector. Some of the advantages *vs.* other encapsulation techniques that have encouraged research efforts using electrohydrodynamic processes include the fact that no high temperatures are required for the drying of the materials, as the whipping of the polymer jet caused by the high voltage application causes solvent evaporation during the flight towards the collector (López-Rubio, Sánchez, Sanz, & Lagaron, 2009). This is especially interesting for the food industry, where the most widely used microencapsulation technology is spray-drying (Kwak, 2014), and low-temperature alternatives are needed for thermosensitive ingredients. Generally, electrohydrodynamic processing has shown high encapsulation efficiencies and it is a very versatile technique, as the morphology of the obtained structures can be varied by changing solution properties and/or process parameters (Gómez-Mascaraque, Sánchez, & López-Rubio, 2016). In this sense, both fibres or capsules may be obtained mainly by adjusting polymer/biopolymer concentration, being the process named electrospinning and electrospraying, respectively. Moreover, the sizes of the structures obtained are usually in the submicron range, thus giving raise to materials with a very large surface-to-mass ratio and this is also important specifically for food applications, as with these small particle sizes, food texture is not expected to be affected. Furthermore, these techniques are industrially scalable and there are already several companies selling industrial electrospinning equipment with production rates of about 0.2 kg/h and annual throughputs of up to 50x106 m^2 of non-woven nanofibers (Persano, Camposeo, Tekmen, & Pisignano, 2013). The interest in the use of these techniques is also reflected in the publication of several review papers (Alehosseini, Ghorani, Sarabi-

Jamab, & Tucker, 2017; Bhardwaj & Kundu, 2010; Schiffman & Schauer, 2008; Wen, Wen, Zong, Linhardt, & Wu, 2017; Mehta, Haj-Ahmad, Rasekh, Arshad, Smith, van der Merwe, Li, Chang, & Ahmad, 2017), to which the interest readers are directed for more information about the basics of these fascinating technologies.

However, most of the developments have been done using synthetic polymers dissolved in organic solvents, while for food applications, natural polymers and food-grade solvents are a must if aiming to any real technology transfer. In this sense, there are a number of challenges that need to be overcome when developing this type of structures. First of all, many natural biopolymers are polyelectrolytes, having strong intermolecular interactions, which need to be overcome for the subsequent formation of electrospun/electrosprayed structures. Moreover, water is not the ideal solvent for electrohydrodynamic processing since, in comparison with organic solvents, it has a high evaporation temperature and high surface tension. In our group, we have extensively worked in the optimization of the conditions for obtaining electrospinning and electrospraying structures using only food-grade materials and developing strategies to overcome the above-mentioned problems (Aceituno-Medina, López-Rubio, Mendoza, & Lagaron, 2013; Gómez-Mascaraque & López-Rubio, 2016; López-Rubio & Lagaron, 2012; Pérez-Masiá, Lagaron, & Lopez-Rubio, 2014a,b). It should be mentioned, however, that there is not a universal strategy that can be applied for stable processing of biopolymers using food grade solvents, and each biopolymeric solution for bioactive encapsulation needs an individual previous optimization.

Another advantage of this technology, which has been scarcely explored in the food area, is the fact that a coaxial configuration may be used to generate multilayer encapsulation structures, which involve one or more additional protective layers for the bioactive ingredients (Zhang, Yao, Ding, Choi, Ahmad, Chang, & Li, 2017) and the potential to tailor their release kinetics (Bock, Dargaville & Woodruff, 2012). In the coaxial configuration, the compound to be encapsulated is pumped together with a biopolymer solution through an independent circuit and flows through an inner needle

and it is coated with an additional biopolymer layer which is pumped through the external needle of the coaxially mounted system. An scheme of this coaxial configuration is shown in Figure 1. Coaxial electrospraying has already been successfully employed for the encapsulation of bioactive agents for pharmaceutical applications (Xie, Ng, Lee, & Wang, 2008; Kim & Kim, 2010; Nie, Dong, Arifin, Hu, & Wang, 2010; Wu, Liao, Kennedy, Du, Wang, Leong, & Clark, 2010, Rasekh, Ahmad, Cross, Hernández-Gil, Wilton-Ely, & Miller, 2017). However, to the best of our knowledge, there are only a few research works about the development of coaxially electrosprayed microcapsules using all food-grade materials, in which alginate-pectin (Koo, Cha, Song, Chung, & Pan, 2014), dextran and whey protein concentrate (WPC) (Pérez-Masiá, Lagaron, & López-Rubio, 2015) and WPC-gelatin (Gómez-Mascaraque, Ambrosio-Martín, Pérez-Masiá, & López-Rubio, 2017) were used as encapsulation matrices.

Zein and gelatin are two food proteins which have been extensively used for the production of electrospun fibers in recent works (Lu, Ma, Xu, Zhang, Cao, & Guo, 2015; Yao, Zhang, Ahmad, Huang, Li, & Chang, 2018). Moreover, both proteins have previously demonstrated their potential to enhance the stability of sensitive bioactive ingredients when used as uniaxially electrosprayed microencapsulation matrices (Gómez-Mascaraque, Lagaron, & López-Rubio, 2015; Gómez-Mascaraque, Pérez-Masiá, González-Barrio, Periago, & López-Rubio, 2017). In this pioneering work, these two proteins were combined for the first time to develop coaxially electrosprayed capsules with the aim of evaluating the potential of the proposed structures for the encapsulation and protection of bioactive food ingredients, as compared to uniaxially electrosprayed capsules. For this purpose, two model bioactive compounds of different nature, one hydrophilic (the polyphenol epigallocatechin gallate - EGCG) and one hydrophobic (α-linolenic acid - ALA), were incorporated within the developed microstructures. The morphology, encapsulation efficiency and protection ability of the developed structures were evaluated.

2. MATERIALS AND METHODS

2.1. Materials

The zein prolamine Z3652 grade and type A gelatine from pig's skin, with 175 g Bloom of gel strength were obtained from Sigma-Aldrich. The α-linolenic acid (ALA), epigallocatechin gallate (EGCG), the diammonium salt of 2,2'-azino-bis(3-etylbenzothiazolin-6-sulfonic) acid (ABTS), the potassium persulphate ($K_2O_8S_2$) and the potassium bromide of spectrometer degree (KBr) were also acquired from Sigma-Aldrich. The acetic acid 96% (v/v) was obtained from Scharlab, while ethanol 96% (v/v) was obtained from Panreac. Salts used in simulated fluids preparation (KCl, KH_2PO_4, $NaHCO_3$, NaCl, $MgCl_2(H_2O)_6$, $(NH_4)_2CO_3$, $CaCl_2(H_2O)_2$) were obtained from Sigma-Aldrich. Digestive enzymes used for the *in-vitro* digestion tests (pepsin, pancreatin from pig's pancreas) and the biliary salts, were obtained from Sigma-Aldrich. The hydrochloric acid (HCl) and the sodium hydroxide (NaOH) were obtained from Scharlab.

2.2. Preparation of electrospraying solutions

Starting biopolymeric solutions were prepared according to previously optimized systems. In the case of zein, a 12% concentration in an aqueous ethanol solution 85% (v/v) was used, as these conditions had previously shown to be adequate to produce fibre-free, homogeneous electrosprayed structures (Costamagna et al., 2017), while the gelatin solutions were prepared using a slightly modified procedure previously optimized by Gomez-Mascaraque et al. (2017) for coaxially electrosprayed gelatin structures. Briefly, 5% (w/v) gelatin was dissolved in acetic acid 40% (v/v) at 40ºC under magnetic agitation and cooled down to room temperature before processing. For the preparation of the bioactive-containing samples, 10% (w/w) of the model bioactives with respect to the protein weight were directly incorporated during the mixing of the electrospraying solutions that were pumped through the inner needle.

154 2.3. Electrospraying of solutions

155 The solutions were processed by either single needle configuration (using a stainless-
156 steel needle of 0.9 mm of inner diameter), or through coaxial electrospraying through
157 two concentric stainless-steel needles (0.6 and 1.4 mm of inner diameters,
158 respectively) using a homemade electrospinning/electrospraying apparatus, equipped
159 with a variable high-voltage 0-30 kV power supply. Solutions were introduced in 5 mL
160 plastic syringes placed on digital pumps and were pumped at steady flow-rates through
161 PTFE wires connected to the needles. Processed samples were collected on a
162 stainless-steel plate connected to the cathode of the power supply and placed
163 horizontally with respect to the syringe. This horizontal configuration was preferred
164 since it avoids dripping of the solutions on the collector during the initial setup of the
165 process. The obtained capsules were subsequently detached from the collector with a
166 stainless-steel spatula, mixing the obtained powders before sampling to ensure that
167 analysed samples were representative of the whole obtained material.

168 The processing parameters were optimized for each solution, but in general, the
169 voltage was kept between 13 kV and 18 kV and the flow rates were 0.15 mL/h for the
170 single needle configuration and 0.05 mL/h and 0.15mL/h for the inner and outer
171 solutions, respectively, for the coaxial configuration. The distance between the needle
172 and the collector was set at 10 cm based on previous works (Costamagna et al., 2017,
173 Gomez-Mascaraque et al., 2017), and it was enough to achieve solvent evaporation.
174 Regarding the encapsulating matrices, different combinations were used to evaluate
175 the impact of using a double protein coating on the stability of the model bioactive
176 compounds: in the case of the ALA-containing particles, given the solubility of this
177 bioactive compound in ethanol, zein was used as the carrier matrix (Z-ALA) and
178 additional gelatin (GZ-ALA) or zein (ZZ-ALA) coatings were applied using the coaxial
179 configuration. In the case of EGCG, as this catechin is soluble in aqueous solutions,
180 both gelatin and zein (Z-EGCG) were evaluated as carrier matrices and an additional
181 gelatin (GG-EGCG) or zein (GZ-EGCG and ZZ-EGCG) layer was generated through

182 the coaxial configuration. The system of a single gelatin matrix with EGCG was
183 previously evaluated (Gómez-Mascaraque, Lagaron, & López-Rubio, 2015).

184 **Table 1.** List of electrosprayed samples studied in this work.

185

Bioactive compound	Sample code	Configuration	Core solution	Shell solution	Polymer mass ratio (zein/gelatin)	Theoretical bioactive content (%)
α-linolenic acid	Z-ALA	Uniaxial	Zein		100:0	10
	GZ-ALA	Coaxial	Zein	Gelatin	44.4:55.6	10
	ZZ-ALA	Coaxial	Zein	Zein	100:0	10
Epigallocatechin gallate	Z-EGCG	Uniaxial	Zein		100:0	10
	GG-EGCG	Coaxial	Gelatin	Gelatin	0:100	10
	GZ-EGCG	Coaxial	Zein	Gelatin	44.4:55.6	10
	ZZ-EGCG	Coaxial	Zein	Zein	100:0	10

186
187

188 2.4. Fourier transform infrared (FT-IR) analysis of the particles

189 Unloaded and bioactive-containing electrosprayed structures were analysed by FT-IR
190 using a Bruker (Rheinstetten, Germany) FT-IR Tensor 37 equipment in transmission
191 mode. The materials (ca. 1 mg) were mixed with 130 mg of spectroscopic grade
192 potassium bromide and ground to obtain a homogeneous mixture, which was
193 compressed at ca. 150 MPa in a manual hydraulic press to obtain a pellet. FT-IR
194 spectra were obtained by averaging 10 scans at 1 cm^{-1} resolution.

195

196 2.5. Morphological characterization of the particles

197 The morphological characterization of the electrosprayed particles was carried out by
198 scanning electron microscopy (SEM) on a Hitachi microscope S-4800 model, at an
199 accelerating voltage of 10 kV, a working distance of 8-12 mm and a magnification of
200 10000x. Prior to sample examination, the electrosprayed structures were sputter-
201 coated with a gold-palladium mixture. Microparticles diameters were measured from
202 the SEM micrographs in their original magnification using the ImageJ software. Size
203 distributions were obtained from a minimum of 200 measurements per image.

204

205 2.6. Encapsulation efficiency

206 The encapsulation efficiency (EE) of the loaded microparticles was determined using
207 infrared spectroscopy (FT-IR). Calibration curves were obtained (R^2 between 0.988 and
208 0.998 for the various protein-bioactive blends) by preparing physical mixtures of the
209 encapsulating matrices and the bioactive compounds at different concentrations of the
210 latter (0, 5, 10 and 15% w/w). Specifically, the bands considered for carrying out the
211 calibration curves were the maximum absorbances of the characteristic bands of the
212 bioactive compounds at ~3010 cm^{-1} (for ALA), and at 1039 cm^{-1} (attributed to EGCG),
213 relative to the maximum absorbances of the bands from the encapsulating matrices at
214 1538 cm^{-1} (for gelatin) and at 1542 cm^{-1} (for zein). These were plotted against the
215 bioactive concentration and the bioactive content was obtained by interpolating from

the linear calibration equations. The encapsulation efficiency (EE) in the different systems was then calculated using Eq. (1):

$$EE(\%) = \frac{Actual\ bioactive\ content\ in\ the\ microcapsules}{Theoretical\ bioactive\ content\ in\ the\ microcapsules} \times 100 \qquad \text{Eq. (1)}$$

2.7. *In-vitro* antioxidant activity of EGCG

To estimate the antioxidant activity of both encapsulated and free EGCG, the $ABTS^{+\cdot}$ radical scavenging assay was performed following a protocol adapted from Re et al. (1999). In brief, a stock solution of $ABTS^{+\cdot}$ was prepared by reacting ABTS with potassium persulfate (7 mM and 2.5 mM in distilled water, respectively) and letting the solution in agitation for 24 hours in the dark at room temperature. This solution was then diluted with a 1:2 v/v mixture containing acetic acid 20% v/v and ethanol 96% (solvent conditions where the different microparticles were completely dissolved) until getting an absorbance of 0.7 ± 0.02 at 734 nm.

Subsequently, solutions of free and encapsulated EGCG (5 mM and 0.25 mM of EGCG, respectively) were prepared in the previously mentioned acetic acid-ethanol mixture. In the case of the capsules, to facilitate the dissolution of the matrices and facilitate the complete release of EGCG from the microparticles, the solvent needed to dissolve the external coating was first used and subsequently blended with the other one, always keeping the same proportion. Then, the stock solution from the free EGCG was diluted 20-fold to have the same starting concentration. 10 µL of diluted sample solution were added to 1 mL of diluted $ABTS^{\bullet+}$, and the absorbance at 734 nm was measured at room temperature 1 min after initial mixing. The radical scavenging activity (RSA), expressed as the percentage of reduction of the absorbance at 734 nm after sample addition, was calculated using Eq. (2):

$$RSA\ (\%) = \frac{A_0 - A_1}{A_0} \times 100 \qquad \text{Eq. (2)}$$

Where A_0 and A_1 are the absorbances at 734 nm of $ABTS^{+\bullet}$ before and 1 min after addition of the antioxidant samples, respectively.

Experiments were performed on a Shanghai Spectrum spectrophotometer model SP-2000UV (Shanghai, China), at least in triplicate. Solvent blanks were also run in each assay. The unloaded electrosprayed microparticles were also evaluated (same particle concentration as in loaded samples) to take into account the potential antioxidant activity of the encapsulation matrices.

2.8. Monitoring of ALA oxidation

For the monitoring of the oxidative stability of ALA-loaded microparticles, samples were subjected to accelerated oxidation conditions by thermal treatment at 80ºC, and attenuated total reflection (ATR)-FTIR spectra were obtained after selected time intervals. For the evaluation of the oxidative stability of the bioactive compound included in the microparticles, these were placed in the GoldenGate accessory from Specac Ltd. (Orpington, U.K.) coupled to the FTIR system, and the absorbance intensity of the band at ~3010 cm^{-1}, corresponding to ALA, was measured. The decrease in the relative intensity of the aforementioned band was related to the extent of ALA degradation within the capsules or in its free form, as previously reported (Gomez-Mascaraque & Lopez-Rubio, 2016).

2.9. Assessment of EGCG bioaccessibility

For the assessment of EGCG bioaccessibility, suspensions (40 mg/mL) of the loaded microparticles and solutions (4 mg/mL) of free EGCG in distilled water were subjected to an *in-vitro* digestion process following the standardized static *in-vitro* digestion protocol described by Minekus et al. (2014). The solutions for the simulated salivary

fluid (SSF), simulated gastric fluid (SGF), and simulated intestinal fluid (SIF) were prepared according to the harmonized compositions (Minekus et al., 2014). Briefly, during the oral phase, the suspensions were mixed with SSF (50:50 v/v) and incubated at 37ºC for 2 min under agitation in a thermostatic bath. In the gastric phase, the oral digesta was mixed with SGF (50:50 v/v) and porcine pepsin (2000 U/mL), and incubated at 37ºC for 2 h under agitation. In the duodenal phase, the gastric digesta was mixed with SIF (50:50 v/v), porcine bile extract (10 mM) and porcine pancreatin (100 U/mL of trypsin activity), and incubated at 37ºC for 2 h under agitation. The pH was adjusted to 7, 3, and 7 in the oral, gastric and duodenal phases, respectively. After the duodenal phase, the protease inhibitor Pefabloc® (1mM) was added. Aliquots were collected after the gastric and the duodenal phases and snap-frozen in liquid nitrogen immediately. The antioxidant activity of the digestas was estimated after centrifugation by means of the $ABTS^{+\bullet}$ assay previously described, as an indirect assessment of the bioaccessibility of EGCG after digestion.

2.10. Statistical analysis

Results were analysed using IBM SPSS Statistics software (v.23) (IBM Corp., USA). The significance of the differences observed between samples was assessed through two-sided t-tests at $p < 0.05$.

3. RESULTS AND DISCUSSION

3.1. Morphology and size distribution of microparticles

Scanning electron microscopy (SEM) was used to characterize the morphology of the different microparticles obtained. An interesting aspect of the electrospraying technique is that it is able to produce smaller particles than other common encapsulation techniques used in the food industry, such as spray-drying, despite requiring higher biopolymer concentrations for processing. In this work, simple matrix type zein microcapsules were produced using the uniaxial configuration, while the coaxial configuration was used to develop more complex core-shell structures by incorporating an additional protein (zein or gelatin) layer. In Figure 2, it can be seen that, in accordance to previous studies, zein microcapsules displayed shrunken-like structures, attributed to the high volatility of ethanol which causes a rapid evaporation of the solvent in the zein solutions, causing the collapse of the structures (Costamagna et al., 2017). Incorporation of the model bioactives (ALA and EGCG) or of an additional zein layer through coaxial electrospraying, did not significantly affect the morphology of the structures as observed in Figure 2. Interestingly, neither the capsule sizes were significantly modified, being most of the structures obtained in the submicron size.

In contrast, the microparticles containing gelatin displayed different morphologies depending on the composition of the capsules. In general, an increase in average size and the presence of residual fibrils were observed in the gelatin-containing structures. Moreover, a greater heterogeneity both in morphology and sizes was observed in these latter structures. It should be emphasized, that in the specific case of the hybrid gelatin-zein structures, different solvent media were used for the processing of each biopolymer, further complicating the electrospraying process.

3.2. Chemical characterization

Infrared spectroscopy was used to investigate potential interactions between the processed matrices. Moreover, the infrared spectra of the loaded microparticles were

318 compared to those of the pure proteins (gelatin and zein) and model bioactive
319 molecules (ALA and EGCG). The spectrum of the commercial proteins (both gelatin
320 and zein) (cf. Figure 3A) showed their characteristic bands centred at ~3430 cm^{-1}
321 (Amide A, NH bond stretching), ~1655 cm^{-1} (Amide I, C=O and CN stretching), ~1540
322 cm^{-1} (Amide II, N-H bending) and ~1243 cm^{-1} (Amide III, C-N stretching). The spectral
323 bands observed at ~2960 cm^{-1} and ~2930 cm^{-1} correspond to CH_2 asymmetric and
324 symmetric stretching vibrations, respectively, mainly from the glycine backbone and
325 proline side-chains (Gómez-Mascaraque, Lagaron, & López-Rubio, 2015; Moomand &
326 Lim, 2014a). Electrohydrodynamic processes induce molecular organization as it has
327 been previously observed (Pérez-Masiá et al., 2014a) and, thus, when comparing the
328 spectra from the starting unprocessed materials with those from the electrosprayed
329 samples, the spectral bands in the latter ones appear much more defined (cf. Figure
330 3A). The most relevant change was observed in the OH and NH stretching region
331 centred around 3400 cm^{-1}. There appear to be significantly less free OH groups,
332 suggesting that electrospraying promotes biopolymer entanglements via hydrogen
333 bonds. Moreover, the amide A band from both proteins shifted to lower wavelengths,
334 which has been previously correlated to hydrogen bond formation via the N-H groups
335 of the peptides (Gómez-Mascaraque et al., 2015). Coaxially combining gelatin and zein
336 (upper spectrum in Figure 3A), results in an intermediate infrared profile, in which no
337 significant shifts were observed which preclude from ascribing any specific interaction
338 between both matrices.
339 When comparing the unloaded electrosprayed samples with the particles containing
340 the hydrophilic bioactive (i.e. EGCG), several bands related to the presence of the
341 bioactive are apparent (see arrows in Figure 3B). Specifically, the spectrum of
342 commercial EGCG (upper spectrum in Figure 3B) showed the OH stretching band at
343 ~3360 cm^{-1} and other characteristic bands mostly related to stretching and deformation
344 vibrations of the aromatic groups as previously reported (Robb, Geldart, Seelenbinder,

345 & Brown, 2002; Gomez-Mascaraque et al., 2015). It should be noted that, despite
346 having the same EGCG theoretical content, the infrared spectrum from the coaxial
347 loaded G-G particles, showed more intense EGCG bands, suggesting that a greater
348 encapsulation efficiency was achieved in this case, as it will be further confirmed
349 below. Slight shifts were observed in some of the bands from the polyphenol (for
350 instance, the band at 1042 cm^{-1} shifted to 1038 cm^{-1} in the capsules), which suggest
351 interactions between the polyphenols and the protein matrices as previously described
352 (Li, Lim, & Kakuda, 2009). Further changes in the spectra related to interactions
353 between the protein matrices in the particles and the EGCG were shifts in the Amide A
354 (around 3400 cm^{-1}) and Amide III (around 1245 cm^{-1}) bands towards lower
355 wavenumbers, suggesting hydrogen bonding interactions between the matrix and the
356 bioactive molecules. These interactions might contribute to the stabilization of the
357 bioactive compound as previously reported (Gómez-Mascaraque et al., 2015).
358 Regarding the ALA-loaded structures, the presence of the hydrophobic bioactive was
359 also apparent in the infrared spectra (see arrows in Figure 3C). The IR spectrum of the
360 commercial bioactive showed its most characteristic vibrational bands centred at 3013
361 cm^{-1} (stretching of cis-alkene groups in PUFAs) and 1711 cm^{-1} (C=O stretching in fatty
362 acids) (Moomand & Lim, 2014b). Other relevant bands of ALA were found at 2965,
363 2932 and 2856 cm^{-1} and are ascribed to the methyl asymmetrical stretching, the
364 methylene asymmetrical stretching and the methylene symmetrical stretching
365 vibrations, respectively (Guillen & Cabo, 1997). The main spectral changes upon ALA
366 incorporation were also observed in the OH and NH stretching region centred around
367 3400 cm^{-1}. While a broadening of this band was observed in the zein structures, this
368 spectral region considerably became narrower for the hybrid G-Z structures. This could
369 be explained by the different aminoacid composition of both proteins, being zein
370 considered a rather hydrophobic protein. Incorporation of the bioactive within the zein
371 matrix apparently leads to some conformational change in the protein, in which the
372 most hydrophobic aminoacids would be weakly interacting with ALA and exposing

more hydrophilic aminoacids, thus giving rise to more hydroxyl groups available. In the hybrid G-Z structures, these hydroxyl groups would interact with those from the gelatin and, as a consequence, a narrower band is observed.

3.3 Encapsulation efficiency

Encapsulation efficiency was determined through infrared spectroscopy, using calibration curves previously obtained for each microparticle composition. The results are shown in Figure 4.

The encapsulation efficiency of ALA-loaded microparticles was significantly high for the three different matrices explored. Interestingly, the coaxial systems were able to trap a greater amount of the bioactive compound, being the formulation with a double zein layer the optimal one in terms of encapsulation efficiency (see Figure 4A). As demonstrated in the previous FTIR section, hydrophobic interactions may be established between the more hydrophobic protein zein and ALA, thus contributing to this increase in encapsulation efficiency.

In the case of EGCG, similar encapsulation efficiencies were observed for the simple zein structures and for the coaxial ones consisting of gelatin-zein and zein-zein. In contrast, the coaxial gelatin structure seemed to have an excellent encapsulation efficiency, significantly greater than that of the other three systems. This could be correlated to the more acidic character of the gelatin solutions, which were prepared in acetic acid-containing aqueous media. Therefore, even though the binding between polyphenols and proteins have been mainly ascribed to hydrophobic interactions (Jakobek, 2015) and it is known that zein, given its aminoacid composition, has a much more hydrophobic character (Singh, Singh, Kaur, & Bakshi, 2012), the greater stability of EGCG in acidic media could result in the observed greater encapsulation efficiency. This better performance of the coaxial GG microcapsules in terms of encapsulation efficiency was confirmed by measuring the *in-vitro* antioxidant activity using the ABTS+· assay (cf. Figure 5).

As observed in Figure 5, the coaxial GG microparticles displayed a significantly higher antioxidant capacity than the microcapsules with zein, thus confirming the FTIR results and suggesting again the greater solubility of this bioactive compound in the gelatin matrix (Gómez-Mascaraque et al., 2015).

3.4 Monitoring ALA degradation

The thermal stability of ALA in the different encapsulation structures was evaluated through FTIR, exposing the samples to 80ºC and quantifying the decrease in the ALA characteristic absorption band at 3010 cm^{-1} as previously reported (Gomez-Mascaraque & López-Rubio, 2016). The results were compared with its stability in free form and are compiled in Figure 6.

From this figure, it can be clearly observed that non-encapsulated ALA is very prone to degradation upon temperature exposure, as 95% of the compound was degraded after 400 minutes of thermal treatment at 80ºC. In contrast, a great stability is achieved upon encapsulation, as previously demonstrated using a number of protein matrices (Gomez-Mascaraque & López-Rubio, 2016). However, while no differences were observed between the simple and coaxial zein-based matrices, combining gelatin and zein in a coaxial structure resulted in a better stability of the compound. This could be ascribed to the lower affinity of ALA with gelatin, which would result in less bioactive molecules exposed in the surface of the capsules (as gelatin was used as the external protective layer). Therefore, while having lower encapsulation efficiency than its counterpart with only zein, this hybrid coaxial GZ structure was the optimal one in terms of protection. In the case of the zein-based structures, given their higher affinity to this hydrophobic bioactive, it is hypothesised that part of the bioactive would be closer to the external surface of the microparticles, thus being more sensitive to degradation.

3.5 Evaluation of antioxidant capacity after *in-vitro* digestion

The $ABTS^{+\cdot}$ assay was used to evaluate the antioxidant capacity of the digestas from the EGCG-loaded microcapsules in comparison to the activity of free EGCG. The results are shown in Figure 7.

In agreement with previous studies (Gómez-Mascaraque, Soler, & López-Rubio, 2016) it was observed that free EGCG showed a good antioxidant activity after the gastric phase, as the catechin more stable in acid conditions such as those found in the stomach, but a considerable loss of antioxidant capacity was seen after the intestinal phase, which may be ascribed to the degradation of the compound at the higher pH of the duodenum. In general, in Figure 7 it is also observed that the antioxidant capacity of the loaded capsules after the gastric phase was significantly lower than that of the free compound. It has been previously observed that polyphenols are able to interact with proteins and, thus, a gradual release in aqueous media has been observed (Gómez-Mascaraque et al., 2015). Therefore, it is reasonable to think that the antioxidant capacity observed is due to the amount of EGCG released from the different encapsulation structures after this gastric phase. The lowest release corresponds to the simple zein structure, given the very low solubility of this protein in water. In contrast, after the intestinal phase, the antioxidant capacity significantly increased for most of the systems developed, which may be due to the combination of both the partial digestion of the protein matrices and the diffusion of the compound. Therefore, in contrast with the unprotected EGCG, the different encapsulation structures exerted a protective effect during the intestinal phase of the in-vitro digestion process. Remarkably, the coaxial G-G structure, displayed a similar antioxidant capacity in comparison with the free EGCG after the gastric phase, explained by the solubilisation of the gelatin in acidic media, thus facilitating EGCG release. However, a protective effect was observed during the intestinal phase, which could be ascribed to soluble complexes of the catechin and gelatin which provide a protective effect during

long hours, even though a rapid release from the structures takes place, as previously reported (Bandyopadhyay, Ghosh, & Ghosh, 2012; Gómez-Mascaraque et al., 2015).

4. CONCLUSIONS

This work has demonstrated the potential of coaxial electrospraying for the development of encapsulation structures with enhanced bioactive protection ability using only food-grade materials and solvents. Different combinations of two proteins (zein - Z and gelatin – G) were used and the structures were loaded with two model bioactive compounds: a hydrophilic polyphenol (epigallocatechin gallate – EGCG) and a hydrophobic fatty acid (α-linolenic acid – ALA). Aqueous-based solutions were implemented for stable capsule production and the microstructure of the capsules varied with composition, although capsule sizes remained in the submicron range. Encapsulation efficiency was seen to be dependent on the chemical compatibility between the bioactive and matrix materials. The coaxial systems showed improved performance in terms of bioactive protection as quantified through thermal degradation assays (in the case of ALA) and antioxidant properties after *in-vitro* digestion (in the case of EGCG).

ACKNOWLEDGMENTS

L. G. Gómez-Mascaraque, M. Martinez-Sanz and M. J. Fabra are recipients of a predoctoral (BES-2013-065883), Juan de la Cierva (IJCI-2015-23389) and Ramón y Cajal (RYC-2014-158) contracts from the Spanish Ministry of Economy, Industry and Competitiveness (MINECO), respectively. The authors would like to thank the Spanish MINECO project AGL2015-63855-C2-1-R for financial support.

ABBREVIATIONS

FT-IR, Fourier transform infrared spectroscopy; Z, zein; G, gelatin; EGCG, epigallocatechin gallate; ALA, α-linolenic acid; PUFAs, polyunsaturated fatty acids; PTFE, Polytetrafluoroethylene.

REFERENCES

Aceituno-Medina, M., López-Rubio, A., Mendoza, S., & Lagaron, J.M. (2013). Development of novel ultrathin structures based in amaranth (*Amaranthus hypochondriacus*) protein isolate through electrospinning. *Food Hydrocolloids, 31*, 289-298.

Alehosseini, A., Ghorani, B., Sarabi-Jamab, M., Tucker, N. (2017). Principles of electrospraying: A new approach in protection of bioactive compounds in foods. Critical Reviews in Food Science and Nutrition, DOI: 10.1080/10408398.2017.1323723.

Bandyopadhyay, P., Ghosh, A.K., & Ghosh, C. (2012). Recent developments on polyphenol–protein interactions: effects on tea and coffee taste, antioxidant properties and the digestive system. *Food & function, 3*, 592-605.

Bhardwaj, N. & Kundu, S.C. (2010). Electrospinning: A fascinating fiber fabrication technique. *Biotechnology Advances, 28*, 325-347.

Bock, N., Dargaville, T. R., & Woodruff, M. A. (2012). Electrospraying of polymers with therapeutic molecules: State of the art. *Progress in Polymer Science*, 37(11), 1510–1551.

Costamagna, M.S., Gómez-Mascaraque, L.G., Zampini, I.C., Alberto, M.R., Pérez, J., López-Rubio, A., & Isla, M.I. (2017). Microencapsulated chañar phenolics: A potential ingredient for functional foods development. *Journal of Functional Foods, 37*, 523-530.

Gómez-Mascaraque, L.G., Ambrosio-Martín, J., Pérez-Masiá, R., & López-Rubio, A. (2017). Impact of acetic acid on the survival of L. plantarum upon microencapsulation by coaxial electrospraying. *Journal of Healthcare Engineering, 2017*, 4698079.

Gómez-Mascaraque, L.G., Lagaron, J.M., & López-Rubio, A. (2015). Electrosprayed gelatin submicroparticles as edible carriers for the encapsulation of polyphenols of interest in functional foods. *Food Hydrocolloids, 49*, 42-52.

Gómez-Mascaraque, L.G. & López-Rubio, A. (2016). Protein-based emulsion electrosprayed micro- and submicroparticles for the encapsulation and stabilization of

511 thermosensitive hydrophobic bioactives. *Journal of Colloid and Interface Science, 465*,
512 259-270.
513 Gómez-Mascaraque, L.G., Pérez-Masiá, R., González-Barrio, R., Periago, M. J., &
514 López-Rubio, A. (2017). Potential of microencapsulation through emulsion-
515 electrospraying to improve the bioaccessibility of β-carotene. *Food hydrocolloids, 73*, 1-
516 12.
517 Gómez-Mascaraque, L.G., Sánchez, G., & López-Rubio, A. (2016). Impact of
518 molecular weight on the formation of electrosprayed chitosan microcapsules as
519 delivery vehicles for bioactive compounds. *Carbohydrate Polymers, 150*, 121-130.
520 Gómez-Mascaraque, L.G., Soler, C., & López-Rubio, A. (2016). Stability and
521 bioaccessibility of EGCG within edible micro-hydrogels. Chitosan vs. gelatin, a
522 comparative study. *Food hydrocolloids, 61*, 128-138.
523 Guillen, M. & Cabo, N. (1997). Characterization of edible oils and lard by Fourier
524 transform infrared spectroscopy. Relationships between composition and
525 frequency of concrete bands in the fingerprint region. *Journal of the American Oil*
526 *Chemical Society, 74*, 1281–1286.
527 Jakobek,L. (2015). Interactions of polyphenols with carbohydrates, lipids and proteins.
528 *Food Chemistry, 175,* 556–567.
529 Kim, W., & Kim, S. S. (2010). Multishell encapsulation using a triple coaxial
530 electrospray system. *Analytical Chemistry*, 82(11), 4644–4647.
531 Koo, S. Y., Cha, K. H., Song, D.-G., Chung, D., & Pan, C.-H. (2014).
532 Microencapsulation of peppermint oil in an alginate–pectin matrix using a coaxial
533 electrospray system. *International Journal of Food Science and Technology*, 49(3),
534 733–739.
535 Kwak, H.-S. (2014). Overview of nano-and microencapsulation for foods. *Nano-and*
536 *Microencapsulation for Foods*, 1-14.
537 Li, Y., Lim, T., & Kakuda, Y. (2009). Electrospun zein fibers as carriers to stabilize (-)-
538 epigallocatechin gallate. *Journal of Food Science, 74*, 233-240.

López-Rubio, A. & Lagaron, J.M. (2012). Whey protein capsules obtained through electrospraying for the encapsulation of bioactives. *Innovative Food Science and Emerging Technologies, 13*, 200-206.

López-Rubio, A., Sánchez, E., Sanz, Y., & Lagaron, J.M. (2009). Encapsulation of living bifidobacteria in ultrathin PVOH electrospun fibers. *Biomacromolecules, 10*, 2823-2829.

Lu, W., Ma, M., Xu, H., Zhang, B., Cao, X., & Guo, Y. (2015). Gelatin nanofibers prepared by spiral-electrospinning and cross-linked by vapor and liquid-phase glutaraldehyde. *Materials Letters, 140*, 1-4.

Mehta, P., Haj-Ahmad, R., Rasekh, M., Arshad, M. S., Smith, A., van der Merwe, S. M., Li, X., Chang, M.-W., & Ahmad, Z. (2017). Pharmaceutical and biomaterial engineering via electrohydrodynamic atomization technologies. *Drug Discovery Today*, 22(1), 157-165.

Minekus, M., Alminger, M., Alvito, P., Ballance, S., Bohn, T., Bourlieu, C., Carriere, F., Boutrou, R., Corredig, M., Dupont, D., Dufour, C., Egger, L., Golding, M., Karakaya, S., Kirkhus, B., Le Feunteun, S., Lesmes, U., Macierzanka, A., Mackie, A., Marze, S., McClements, D.J., Menard, O., Recio, I., Santos, C.N., Singh, R.P., Vegarud, G.E., Wickham, M.S.J.,Weitschies, W., & Brodkorb, A. (2014). A standardised static in vitro digestion method suitable for food – an international consensus. *Food & Function, 5*, 1113–1124.

Moomand, K. & Lim, L.-T. (2014a). Properties of encapsulated fish oil in electrospun zein fibres under simulated in vitro conditions. *Food and Bioprocess Technology, 8*, 431-444.

Moomand, K. & Lim, L.-T. (2014b). Oxidative stability of encapsulated fish oil in electrospun zein fibres. *Food Research International, 62*, 523–532.

Nie, H., Dong, Z., Arifin, D. Y., Hu, Y., & Wang, C. H. (2010). Core/shell microspheres via coaxial electrohydrodynamic atomization for sequential and parallel release of drugs. *Journal of Biomedical Materials Research Part A*, 95(3), 709–716.

Pérez-Masiá, R., Lagaron, J.M., & López-Rubio, A. (2014a). Development and optimization of novel encapsulation structures of interest in functional foods through electrospraying. *Food and Bioprocess Technology, 7*, 3236-3245.

Pérez-Masiá, R., Lagaron, J.M., & López-Rubio, A. (2014b). Surfactant-aided electrospraying of low molecular weight carbohydrate polymers from aqueous solutions. *Carbohydrate Polymers, 101*, 249-255.

Pérez-Masiá, R., Lagaron, J. M., & López-Rubio, A. (2015). Morphology and stability of edible lycopene-containing micro- and nanocapsules produced through electrospraying and spray drying. *Food and Bioprocess Technology*, 8(2), 459–470.

Persano, L., Camposeo, A., Tekmen, C. & Pisignano, D. (2013). Industrial upscaling of electrospinning and applications of polymer nanofibers: a review. *Macromolecular Materials and* Engineering, 298(5), 504-520.

Rasekh, M., Ahmad, Z., Cross, R., Hernández-Gil, J., Wilton-Ely, J. D. E. T., & Miller, P. W. (2017). Facile Preparation of Drug-Loaded Tristearin Encapsulated Superparamagnetic Iron Oxide Nanoparticles Using Coaxial Electrospray Processing. *Molecular Pharmaceutics*, 14 (6), 2010-2023.

Re, R., Pellegrini, N., Preteggente, A., Pannala, A., Yang, M., & Rice-Evans, C. (1999). Antioxidant activity applying an improved ABTS radical cation decoloration assay. *Free Radical Biology & Medicine, 26*, 1231-1237.

Robb, C.S., Geldart, S.E., Seelenbinder, J.A., & Brown, P.R. (2002). Analysis of green tea constituents by HPLC-FTIR. *Journal of Liquid Chromatography & Related Technologies, 25*, 787-801.

Schiffman, J.D. & Schauer, C.L. (2008). A review: electrospinning of biopolymer nanofibers and their applications. *Polymer Reviews, 48*, 317-352.

Singh, N., Singh, S., Kaur, A., & Bakshi, M.S. (2012). Zein: Structure, Production, Film Properties and Applications. In M.J. John, & S. Thomas (Eds.), *Natural Polymers: composites* (pp. 204-218). Great Britain: Royal Society of Chemistry.

Wen, P., Wen, Y., Zong, M.-H., Lindhardt, R.J., & Wu, H. (2017). Encapsulation of bioactive compound in electrospun fibers and its potential application. *Journal of Agricultural and Food Chemistry, 65*, 9161-9179.

Wu, Y., Liao, I.-C., Kennedy, S. J., Du, J., Wang, J., Leong, K. W., & Clark, R. L. (2010). Electrosprayed core–shell microspheres for protein delivery. *Chemical Communications*, 46(26), 4743–4745.

Xie, J., Ng, W. J., Lee, L. Y., & Wang, C.-H. (2008). Encapsulation of protein drugs in biodegradable microparticles by co-axial electrospray. *Journal of Colloid and Interface Science*, 317(2), 469–476.

Yao, Z.-C., Zhang, C., Ahmad, Z., Huang, J., Li, J.-S., & Chang, W. (2018). Designer fibers from 2D to 3D – Simultaneous and controlled engineering of morphology, shape and size. *Chemical Engineering Journal, 334*, 89-98.

Zhang, C., Yao, Z.-C., Ding, Q., Choi, J. J., Ahmad, Z., Chang, M.-W., & Li, J.-S. (2017). Tri-Needle Coaxial Electrospray Engineering of Magnetic Polymer Yolk–Shell Particles Possessing Dual-Imaging Modality, Multiagent Compartments, and Trigger Release Potential. *ACS Applied Materials & Interfaces,* 9 (25), 21485-21495.

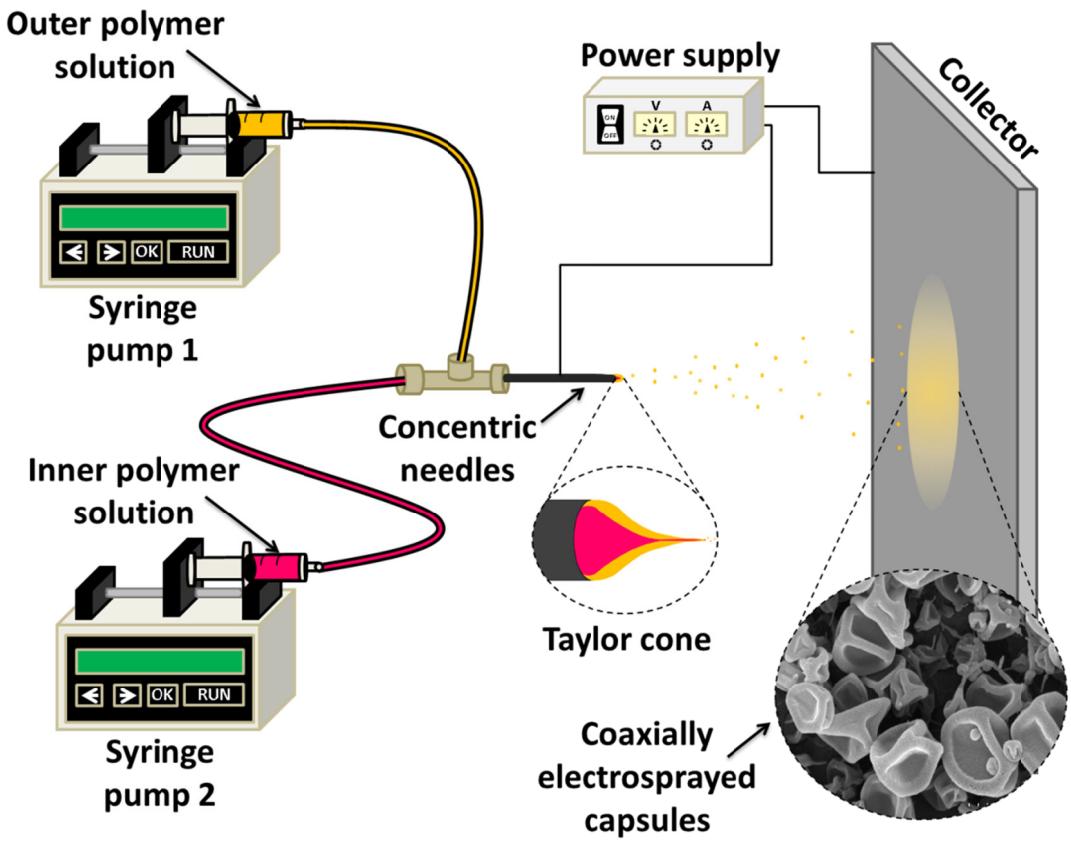

612

613

614 **Figure 1.** Scheme of the coaxial electrospraying configuration.

615

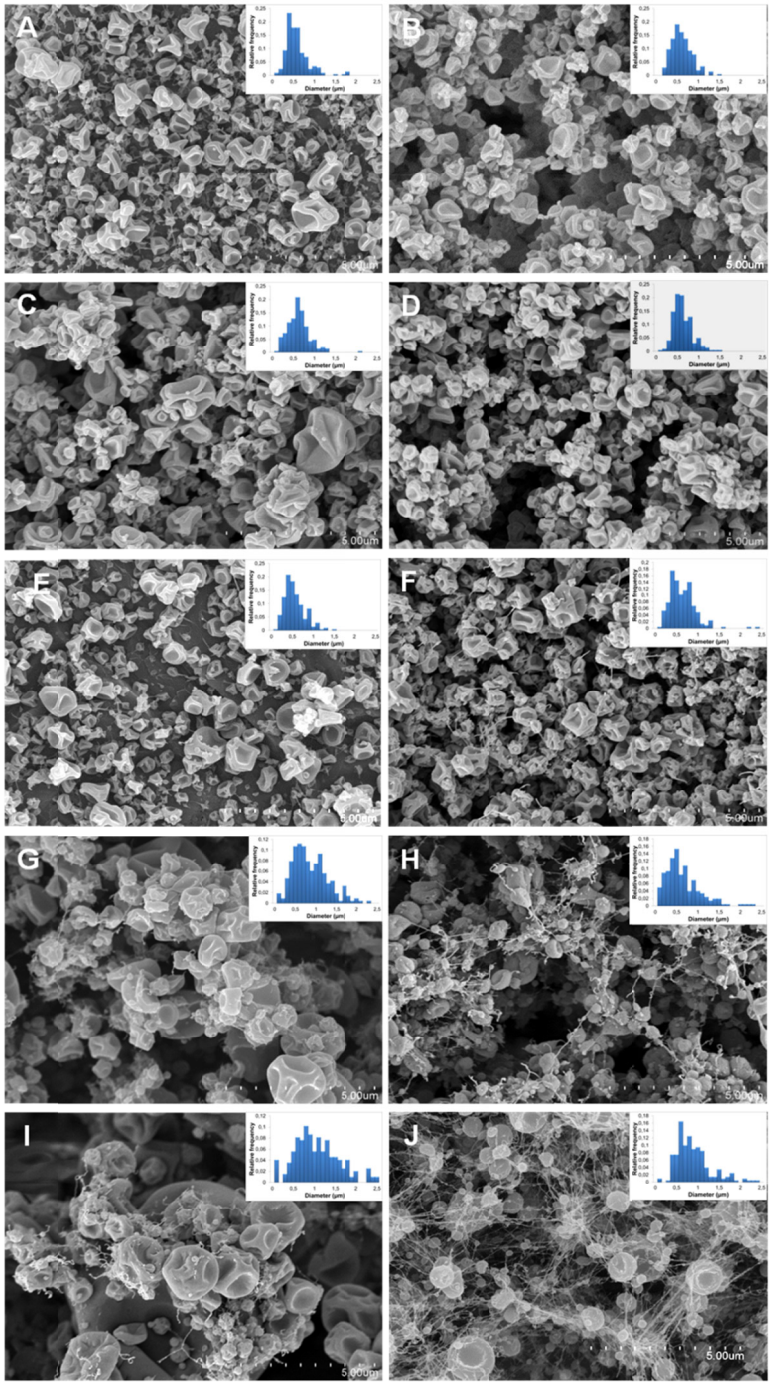

Figure 2. SEM images of electrosprayed microparticles and their size distribution (insets): A) Z (uniaxial); B) Z-ALA (uniaxial); C) ZZ (coaxial); D) ZZ-ALA (coaxial); E) Z-EGCG (uniaxial); F) ZZ-EGCG (coaxial); G) GZ (coaxial); H) GZ-ALA (coaxial); I) GZ-EGCG (coaxial); J) GG-EGCG (coaxial). Scale bars correspond to 5 microns. Abbreviations: Z (zein), G (gelatin), ALA (α-linolenic acid), EGCG (epigallocatechin gallate).

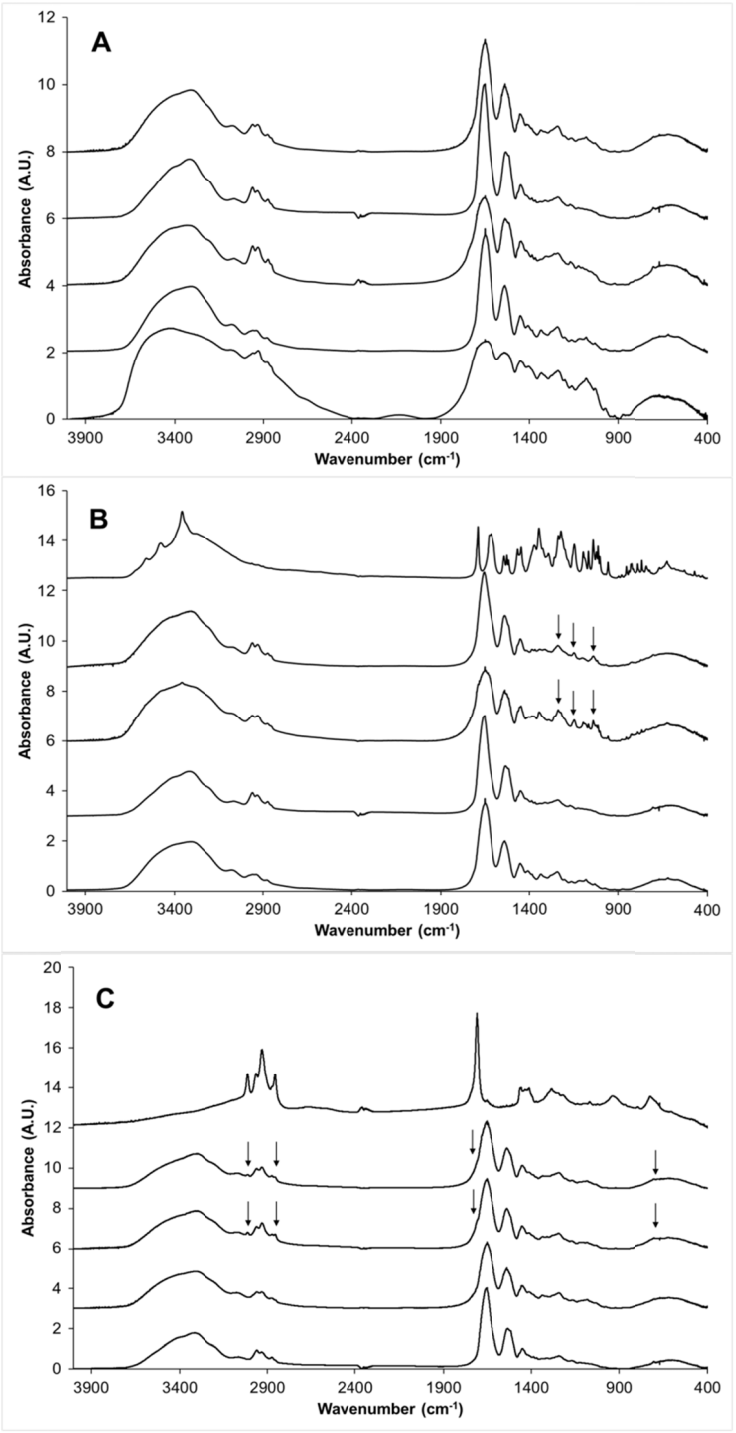

Figure 3. FTIR spectra of the different materials: A) From bottom to the top: Unprocessed gelatin (G); Electrosprayed (ES)-G; Unprocessed zein (Z); ES-Z; ES-GZ. B) From bottom to the top: ES-G; ES-Z; ES-G-G-EGCG; ES-Z-EGCG; EGCG. C) From bottom to the top: ES-Z; ES-GZ; ES-Z-ALA; ES-GZ-ALA; ALA. Arrows point out spectral bands related to the presence of bioactives. Spectra have been offset for clarity.

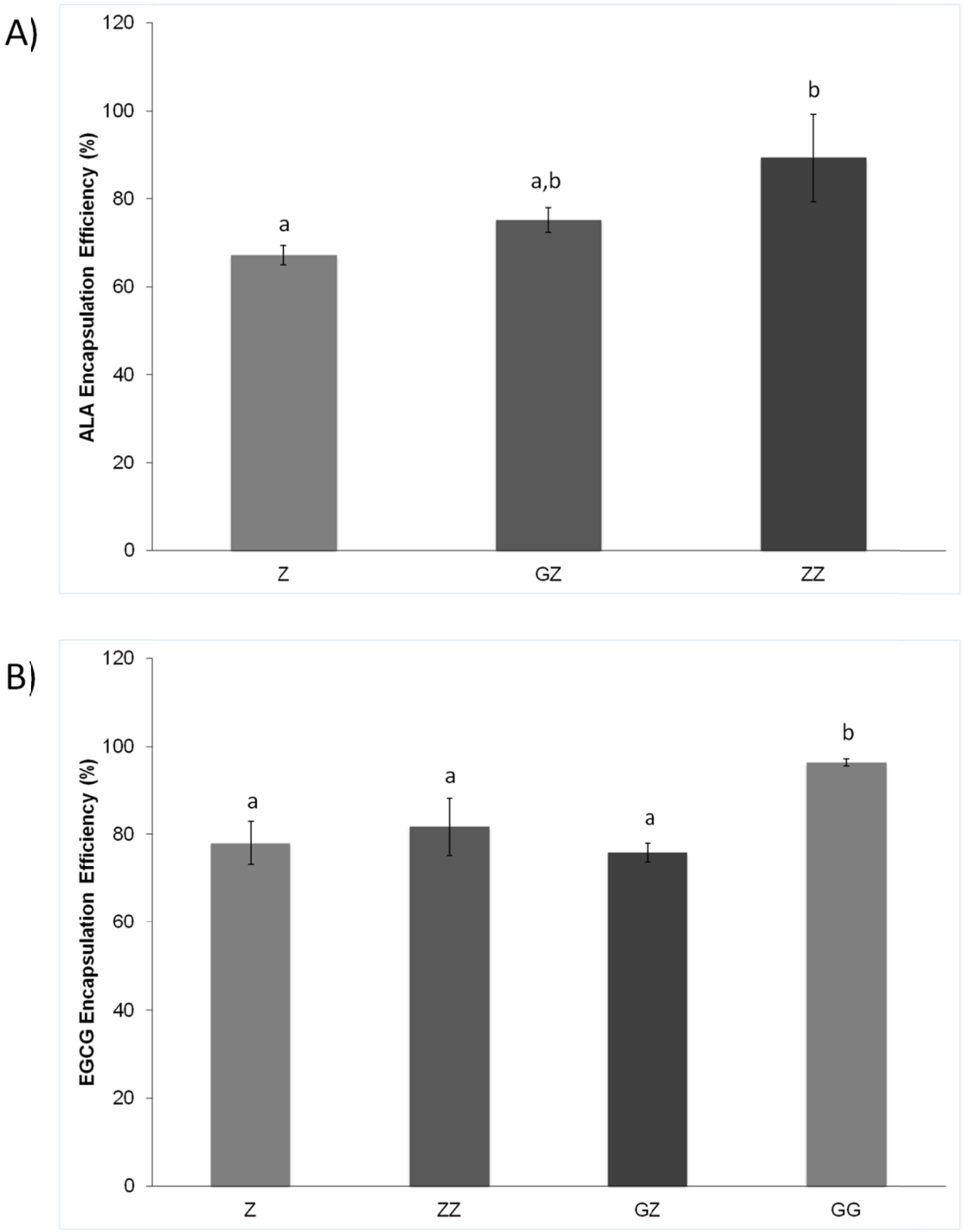

631

632

635 **Figure 4.** Encapsulation efficiency of the different capsules developed containing: A)

636 ALA; B) EGCG. Different letters (a-b) indicate significant differences among the

637 samples.

636

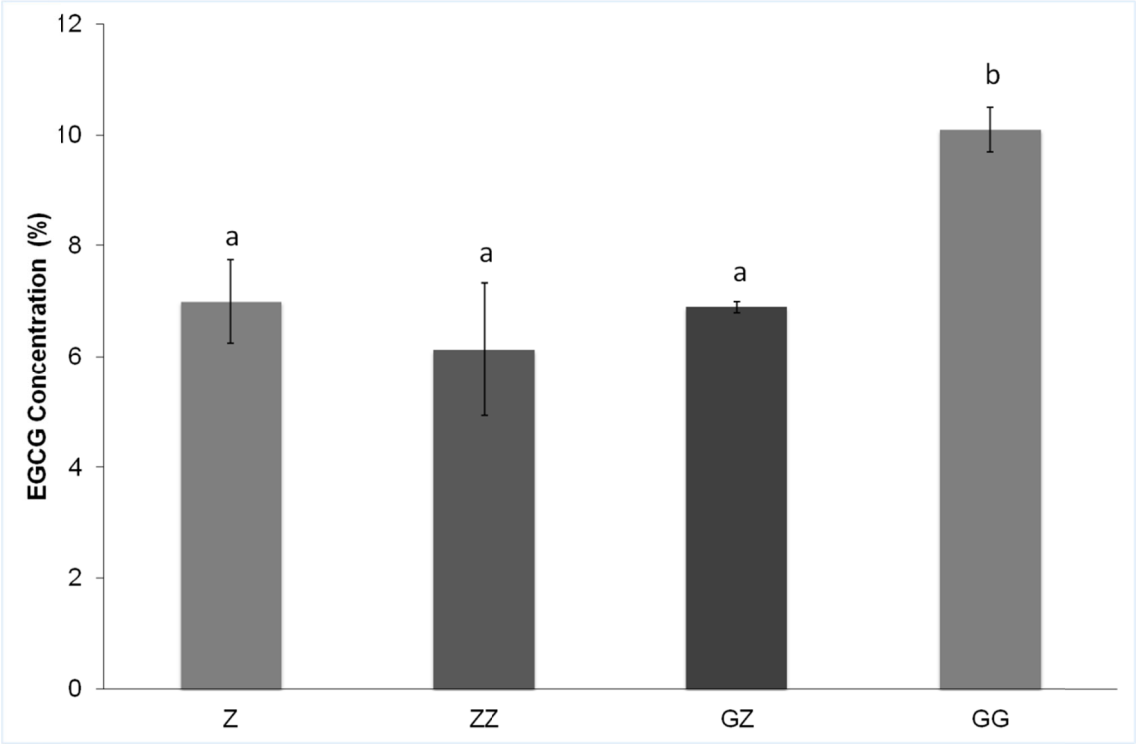

637

638

641 **Figura 5.** EGCG content in microparticles with different matrices, based on its *in-vitro*

642 antioxidant activity. Different letters (a-b) indicate significant differences among the

643 samples.

642

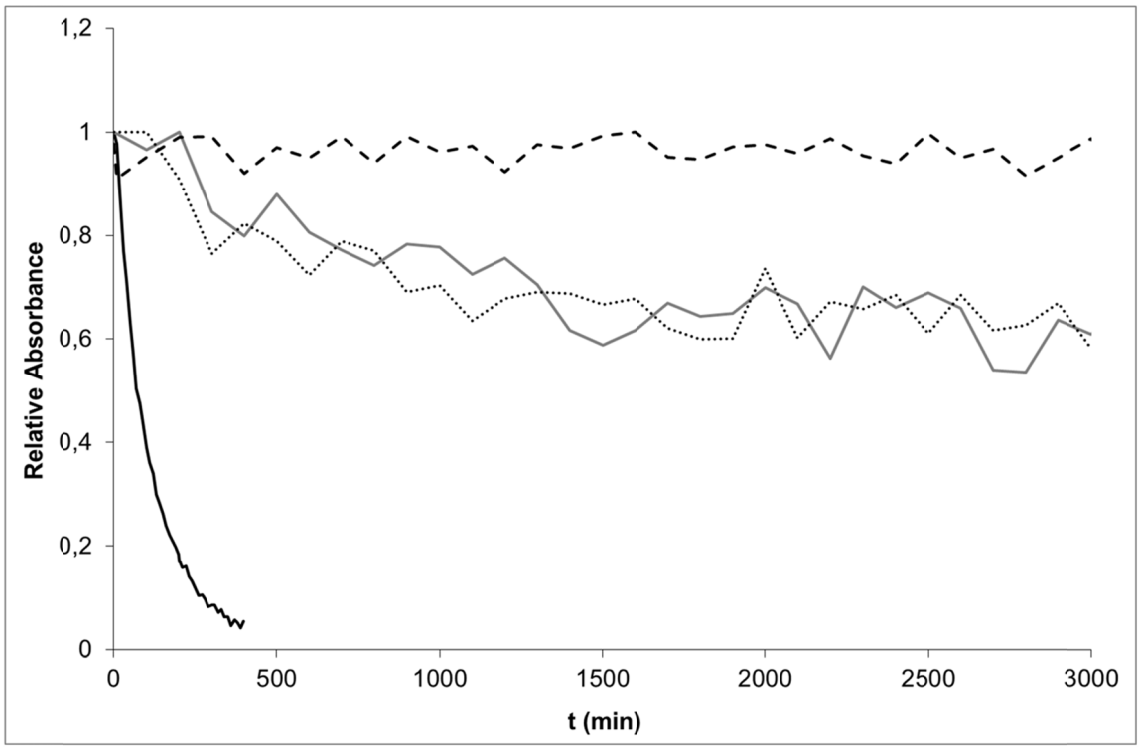

643

646 **Figure 6.** Degradation profiles at 80ºC for unprotected (solid black line) and

647 encapsulated ALA using a single zein (Z) matrix (solid grey line), a coaxial ZZ structure

648 (dotted line) and a coaxial gelatin (G)-Z structure (dashed line).

647

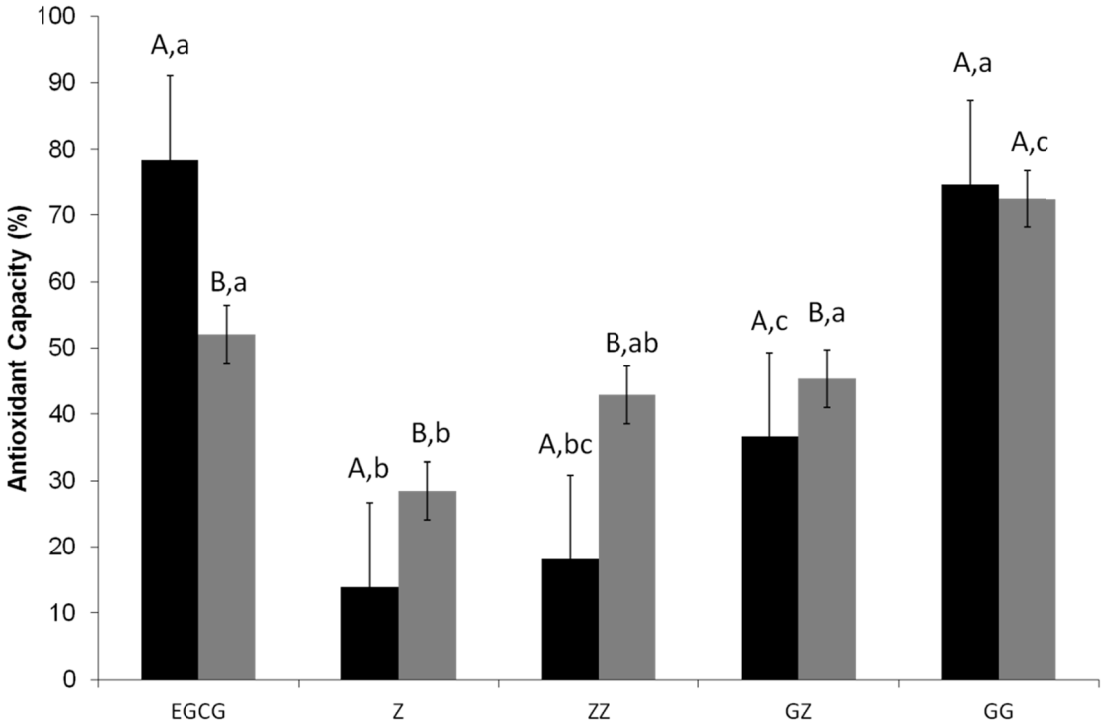

Figure 7. Antioxidant capacity of free EGCG and EGCG encapsulated in zein (Z) or in the coaxial ZZ, gelatin (G)-Z and GG systems after the gastric (black bars) and intestinal (grey bars) phases of an *in-vitro* digestion experiment. Different capital letters (A-B) indicate significant differences between the gastric and the duodenal phases for each sample. Different lower-case letters (a-c) indicate significant differences among the samples for each phase.